

# Header Design for Flow Equalization in Microstructured Reactors

Evgeny V. Rebrov, Ilyas Z. Ismagilov, Rahul P. Ekatpure, Mart H.J.M. de Croon, and Jaap C. Schouten  
Laboratory of Chemical Reactor Engineering, Eindhoven University of Technology, 5600 MB Eindhoven, The Netherlands

DOI 10.1002/aic.11043

Published online November 15, 2006 in Wiley InterScience (www.interscience.wiley.com).

*To enhance the uniformity of fluid flow distribution in microreactors, a header configuration consisting of a cone diffuser connected to a thick-walled screen has been proposed. The thick-walled screen consists of two sections: the upstream section constitutes a set of elongated parallel upstream channels and the downstream section constitutes a set of elongated parallel downstream channels positioned at an angle of 90° with respect to the upstream channels. In this approach the problem of flow equalization reduces to that of flow equalization in the first and second downstream channels of the thick-walled screen. In turn, this requires flow equalization in the corresponding cross sections of the upstream channels. The computational fluid dynamics analysis of the fluid flow maldistribution shows that eight parallel upstream channels with a width of 300–600 μm are required per 1 cm of length for flow equalization. The length to width ratio of these channels has to be >15. The numerical results suggest that the proposed header configuration can effectively improve the performance of the downstream microstructured devices, decreasing the ratio of the maximum flow velocity to the mean flow velocity from 2 to 1.005 for a wide range of Reynolds numbers (0.5–10). © 2006 American Institute of Chemical Engineers AIChE J, 53: 28–38, 2007*

**Keywords:** design, thick-walled screen, flow maldistribution, microreactor, CFD

## Introduction

The demand for high-performance microstructured devices is continuously increasing because of their application in different areas such as high-throughput catalyst testing, kinetic studies of highly exothermic reactions, synthesis and decomposition of hazardous chemicals, and portable hydrogen production. The nonuniformity of fluid flow distribution in the microchannels affects the efficiency of the microreactor. The nonuniformity in the flow distribution is principally attributed to the finite dimensions of the microreactor units, frequently making impossible the use of sufficiently smooth transitions from a cross-sectional shape of the reactor to that of the

upstream and downstream pipes. In large-scale chemical reactors, an additional resistance is usually created by the catalyst layer, which may be considered as a part of the flow distribution system. In microstructured reactors, however, the overall pressure drop over the set of microchannels seldom exceeds 5% of the total pressure in the system. Therefore, uniform distribution of flow can be attained only by special equalizing and distributing devices positioned upstream of the reactor unit. Sometimes, it is also necessary to transform one form of the velocity profile into another.<sup>1</sup>

There has been considerable attention in recent years focused on equalizing the fluid flow distribution in microreactor channels. Commenge et al.<sup>2</sup> developed an approximate pressure drop model to investigate the effect of microchannel geometry parameters on the single-phase fluid flow distribution in a multiplate microreactor. This approximate model, based on the resistive network of ducts, can be used to design optimum plate geometries to achieve uniform flow velocity distribution in downstream microchannels. The results of this model were confirmed by finite-volume calculations. Ajmera et al.<sup>3</sup>

Correspondence concerning this article should be addressed to J. C. Schouten at j.c.schouten@tue.nl.

I. Z. Ismagilov is also affiliated with the Laboratory of Environmental Catalysis, Boreskov Institute of Catalysis SB RAS, Prospekt Akademika Lavrentieva, 5, Novosibirsk, 630090, Russia.

developed a novel design of a silicon cross-flow microreactor for parallel testing of porous supported-catalyst beds. The even flow distribution in individual catalyst beds was achieved by bifurcating the inlet channel into 64 parallel microchannels (tree branching concept). The uniform flow distribution in these channels was validated by flow visualization experiments. The flow distribution within the catalysts bed was also analyzed by 2-D computational fluid dynamics (CFD) calculations. Amador et al.<sup>4</sup> studied manifold structures (consecutive and bifurcation) used for even flow distribution in microchannels. The proposed analytical model, analogous to electrical resistance networks, can be effectively used to study the effect of manufacturing tolerances and channel blockages on the flow distribution in downstream microchannels. A CFD- and finite-element method (FEM)-based analysis of the flow distribution in a plate-fin microdevice was reported in several studies.<sup>5,6</sup> It was shown that the even flow distribution in the branched microchannels of the microdevices and in plate-fin (micro-) heat exchangers<sup>7,8</sup> is profoundly affected by the shape of inlet and outlet manifolds.

The geometric parameters and shapes of the reactor units and of the inlet and the outlet parts are highly varied. Therefore, the methods of fluid flow equalization are also different. Meshes (grids) or screens (perforated sheets, etc.) are usually used for equalizing fluid flow distribution in the reactors. By selection of the density of meshes and the local patches, the necessary degree of flow uniformity can be attained.<sup>9</sup> A sheet screen (grid) is the most effective and simple way to distribute fluid flow equally thorough a whole cross section of the reactor. Such a grid creates additional fluid flow resistances, which are equally distributed across the whole cross section of the reactor. The screen-leveling property depends on its geometrical parameters such as the effective (open) cross section and the thickness of the resistance layer (resulting from screens). The resistance of the grid increases with decreasing effective cross section or with increasing thickness of the resistance layer. These parameters define the drag coefficient of the screen, expressed as

$$\zeta_{sc} = \frac{2\Delta p}{\rho \bar{w}_{sc}^2} \quad (1)$$

where  $\bar{w}_{sc}$  is the average velocity,  $\rho$  is the fluid density, and  $\Delta p$  is pressure drop along the screen. A similar expression can be applied to estimate the resistance of the downstream equipment (such as a microreactor). It is compulsory to use a flow distribution system if the drag coefficient of the resistance layer ( $\zeta$ ) is  $<1000$ .<sup>10</sup>

Importantly, there is a clear difference between planar (or thin-walled) and three-dimensional (thick-walled) screens. The former does not have guiding walls, whereas the latter consists of a number of thick bars, whose thickness in the direction of the fluid flow equals or exceeds the spacing between them. In the case of a thin screen (such as gauze), there is a critical value of  $\zeta_{sc}$  (see Eq. 2) beyond which the degree of fluid flow equalization in a cross section at finite distance downstream from it may considerably differ from the degree of flow spreading upstream of the screen:

$$\zeta_{sc}^{cr} = 3.5 \left( \frac{N_0 A_{sc}}{A_0} - 1 \right) \quad (2)$$

In this expression, also known as Idelchik's correlation,<sup>9</sup>  $N_0$  is the Coriolis's coefficient and  $A_{sc}$  and  $A_0$  are the open cross sections of the screen and the inlet flow duct, respectively.

The internal (hydraulic) diameter of the inlet flow duct of the microreactor is typically between 1 and 4 mm and the inlet duct is sufficiently long, so that at a certain distance from the inlet region of the duct, a constant parabolic velocity profile develops, with maximum at the axis and with zero at the walls:

$$\frac{w}{w_{\max}} = 1 - y^2 \quad (3)$$

It is easy to evaluate the Coriolis coefficient for this case. Assigning the normalized deviation of velocities from the average value as  $\Delta \bar{w} = (\Delta w / \bar{w})$ , it can be derived that

$$N_0 = \frac{1}{A_0} \int_{A_0} (1 + \Delta \bar{w})^3 dA = 1 + \frac{3}{A_0} \int_{A_0} \Delta \bar{w} dA + \frac{3}{A_0} \int_{A_0} \Delta \bar{w}^2 dA + \frac{1}{A_0} \int_{A_0} \Delta \bar{w}^3 dA \quad (4)$$

The second term of this sum equals zero by definition of average velocity, whereas the fourth term is alternating and small, so it can be neglected. Therefore, for a parabolic velocity profile

$$N_0 \approx 1 + \frac{3}{A_0} \int_{A_0} \Delta \bar{w}^2 dA = 1.57 \quad (5)$$

In this way, the critical values of the screen drag coefficient estimated by Eq. 2 are equal to 7.5, 18.5, and 29.5 for  $A_{sc}/A_0$  values of 2, 4, and 6, respectively.

On the other hand, there is an optimum value for the drag coefficient of the flat screen, which can be calculated for  $A_{sc}/A_0 \leq 10$  by the following equation:<sup>9</sup>

$$\zeta_{sc}^{opt} = N_0 \left( \frac{A_{sc}}{A_0} \right)^2 - 1 \quad (6)$$

It is easy to see that for a planar screen the design criterion  $\zeta_{sc}^{opt} < \zeta_{sc}^{cr}$  is satisfied only in a narrow range at  $A_{sc}/A_0 < 2.9$ ; otherwise, planar screens can even amplify the flow nonuniformity downstream of them, giving to the flow profile a distribution that is directly opposite to that of the distribution upstream of the screen.<sup>10,11</sup> Therefore, a planar screen cannot ensure a uniform velocity distribution in a typical range of  $A_{sc}/A_0 > 10$  applied in microreaction technology.

This problem does not exist in the case of thick-walled screens because the degree of velocity equalization is virtually the same at all cross sections downstream from them. In this case, the nature of the distribution of the inlet flow under a given set of flow conditions is a function only of the shapes and geometric parameters of the downstream reactor and the inlet flow duct of the screen. If the shape and parameters are specified, the problem of velocity distributions can be solved in a rather general form without taking into account what chemical or technological process occurs within the downstream reactor.

Problems of flow equalization over the cross section of reactors by screens have been investigated for some time.

Initially, those problems were solved empirically. Riman<sup>12</sup> obtained an expression for the value of the drag coefficient, which ensures the specified degree of flow equalization. An approximate determination of the stream function, whose derivatives satisfy the boundary conditions at the channel walls and at the screen, was performed by Taylor and Batchelor.<sup>13</sup> Riman and Cherepkova<sup>14</sup> proposed a method for calculating the distortion of the velocity profile by bars placed in a tube. However, these problems are solved for high Reynolds (Re) numbers, often corresponding to turbulent flow regime, which is not a case in microstructured reactors.

In this article a study on the performance of the header consisting of a fluid flow diffuser and a thick-walled screen with a thickness of parallel bars in the micrometer range is presented. This type of header can effectively equalize the fluid flow distribution in the plate-type microreactors in the laminar flow regime corresponding to  $Re < 10$ . The study of the fluid flow distribution at the header was investigated by means of the CFD package FLUENT<sup>®</sup> 6.0.<sup>15</sup> This contribution mainly describes the numerical investigation on the effect of the screen configuration parameters on the flow distribution in a downstream microreactor. Results of the experimental validation of the present configuration are presented elsewhere.<sup>16,17</sup>

## Geometry

### Physical model

A schematic view of the header is shown in Figure 1. The header consists of a cone diffuser and a thick-walled screen positioned in front of the microreactor. The thick-walled screen consists of two sections positioned with a  $90^\circ$  turn relative to each other. The upstream section (U) consists of a set of  $m$  elongated parallel upstream channels and the downstream section (D) consists of a set of  $n$  elongated parallel downstream channels positioned at an angle of  $90^\circ$  with respect to the upstream channels. Depending on the number of upstream and downstream channels, the screens will be referred to as  $[m \times n]$  hereafter. The whole geometry is defined by the following parameters: parameter  $a$  is the minimum length between two neighboring downstream channels and parameter  $b$  is the distance in cross-sectional view between a top wall of the first downstream channel and a side wall of the upstream channels. In other words, the value  $b$  is the overhang of the cross section of upstream channels with respect to the cross section of the first downstream channel. Parameter  $c$  is the width of the upstream channels; parameter  $d$  is the height of the downstream channels; parameter  $h$  is the distance between the neighboring upstream channels; parameters  $l_{up}$  and  $l_{down}$  are the lengths of upstream and downstream channels of the screen, respectively; and  $d1$  is the diameter of the channels in the microreactor (R) connected to the downstream channels of the header.  $d1$  is usually equal to or slightly lower than parameter  $d$ , so the distance in the vertical direction between the channels in the microreactor ( $a1$ ) is equal to or slightly higher than distance  $a$ .

In general, the greater the diffuser expansion angle  $\alpha$  (Figure 1), the steeper the velocity drop at the walls of the diffuser and the more elongated is the velocity profile, that is, the higher is the ratio of the maximum velocity to the mean velocity, at the entrance to the upstream channels. At constant inlet conditions and constant relative length of the

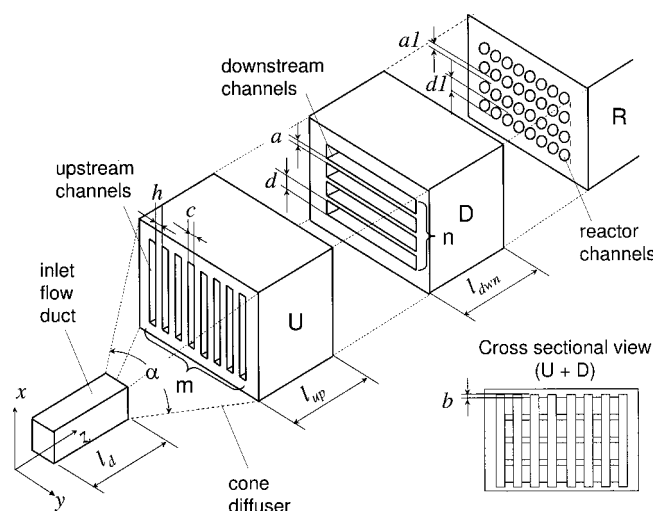


**Figure 1. The header consists of a cone diffuser and a thick-walled screen positioned in front of the microreactor.**

The thick-walled screen consists of two sections positioned with a  $90^\circ$  turn relative to each other. The upstream section (U) consists of a set of  $m$  elongated parallel upstream channels and the downstream section (D) consists of a set of  $n$  elongated parallel downstream channels positioned at an angle of  $90^\circ$  with respect to the upstream channels. Parameter  $a$  is the minimum length between two neighboring downstream channels; parameter  $b$  is the distance in cross-sectional view between a top wall of the first downstream channel and a side wall of the upstream channels; parameter  $c$  is the width of the upstream channels; parameter  $d$  is the height of the downstream channels; parameter  $h$  is the distance between the neighboring upstream channels; parameters  $l_{up}$  and  $l_{down}$  are the lengths of upstream and downstream channels of the screen, respectively.  $d1$  is the diameter of the channels in the microreactor (R) connected to the downstream channels of the header.  $d1$  is usually equal to or slightly lower than distance  $d$ , so the distance in the vertical direction between the channels in the microreactor ( $a1$ ) is equal to or slightly higher than distance  $a$ .

diffuser, there are four principal flow modes, depending on angle  $\alpha$ , of the flow diffuser<sup>18</sup> (Table 1). In microreactors it is desirable to avoid large dead volumes; therefore diffusers of type IV are usually applied. This means that an elongated velocity profile is developed with a ratio of the maximum velocity to the mean velocity  $> 2$  at the entrance to the upstream channels.<sup>18</sup>

### Computational domain

In this work, the CFD code FLUENT<sup>®</sup> 6.0 was used to simulate the fluid flow distribution and pressure drops along the screens. Physical parameters of air [at standard temperature and pressure (STP) conditions] were used throughout this work for definition of the gas-phase properties. The continuity equation and the momentum equation are discretized using a finite-volume method. The semi-implicit SIMPLER algorithm is used in the velocity and pressure conjugated problem. Boundary conditions applied are as follows: inlet fluid Reynolds numbers and outlet pressure are given and no slip occurs on the wall. The convergence criterion is specified to residuals smaller than  $1 \times 10^{-6}$ . The header has two symmetry planes; thus, only one fourth of the screen

**Table 1. Principal Flow Modes at the Outlet of the Flow Diffuser, Depending on the Diffuser Expansion Angle  $\alpha^*$**

	Mode	Diffuser Angle ( $^\circ$ )	Flow Description
I	Separation free diffusers	$\alpha \leq 4$	Stable flow
II	Diffusers with local flow separation	$6 < \alpha \leq 14$	Large unsteady flow detachment
III	Diffusers with significant flow separation	$14 < \alpha \leq 40$	Fully developed flow separation: a large part of the diffuser is occupied by a wide recirculation zone
IV	Diffusers with total flow detachment	$\alpha > 40$	Jet flow: the main stream is separated from the diffuser walls over entire perimeter

\*From Idelchik and Ginzburg.<sup>18</sup>

was modeled. A mesh independency check was performed on the results of the CFD model. Furthermore, the results of the CFD simulations were verified by measuring flow distribution at the outlets of the downstream channels by laser Doppler anemometry (LDA) as described elsewhere.<sup>16</sup> The experimental results showed good agreement with numerical results for a wide range of Re numbers.

The inlet cone diffuser was not taken into the computational domain. However, the inlet Reynolds numbers in the upstream channels of the screen were assigned with three velocity profiles (see Figure 2). In the case of an uneven number of upstream channels, velocity profiles were determined as follows:

(1) Elongated profile with a ratio of the maximum velocity to the mean velocity ( $\bar{w}_{\max}$ ) of 2.0:

$$w_i^{el} = w_{m+1-i}^{el} = 2 \sin^2 \left\{ \frac{[(c+h)(i-1) + \frac{c}{2}] \pi}{(c+h) \frac{m-1}{2} + \frac{c}{2}} \right\} \quad (7)$$

where  $1 \leq i \leq (m+1)/2$ .

(2) Parabolic profile with  $\bar{w}_{\max}$  of 1.5:

$$w_i^{par} = w_{m+1-i}^{par} = 1.5 \left\{ 1 - \left[ \frac{(c+h)(\frac{m+1}{2} - i)}{(c+h) \frac{m-1}{2} + \frac{c}{2}} \right]^2 \right\} \quad (8)$$

where  $1 \leq i \leq (m+1)/2$ .

(3) Uniform profile with  $\bar{w}_{\max}$  of 1.0:

$$w_i^{un} = 1 \quad (9)$$

where  $1 \leq i \leq m$ .

In this way, the mean inlet velocity over all upstream channels is equal in all three cases:

$$\bar{w}^{el} = \bar{w}^{par} = \bar{w}^{un}$$

Similar distributions were used for an even number of upstream channels.

The velocity profile at the each outlet of the downstream channels of the screen was characterized by the flow nonuniformity index, defined as

$$\delta = \frac{100}{\bar{v}} \sqrt{\frac{\sum_{j=1}^n \varepsilon_j^2}{(n-1)}} \quad (\%) \quad (10)$$

where  $\varepsilon_j = v_j - \bar{v}$ ,  $v_j$  is the area average velocity in the outlet channel  $j$  and  $\bar{v}$  is the mean velocity over all outlet channels. It should be noted that  $\bar{v}^{el} = \bar{v}^{par} = \bar{v}^{un}$ . Such a definition of flow nonuniformity also allows us to compare the results obtained at different flow velocities.

Flow nonuniformity was calculated for a  $[45 \times 38]$  screen at several different values of relative length of the upstream channels ( $l_{up}^*$ ) using a parabolic profile at the entrance. Figure 3 demonstrates that the flow nonuniformity starts to increase below  $l_{up}^* = 7.5$ . However, the flow development length is not observed to vary substantially over the range of average flow velocities applied in this study.

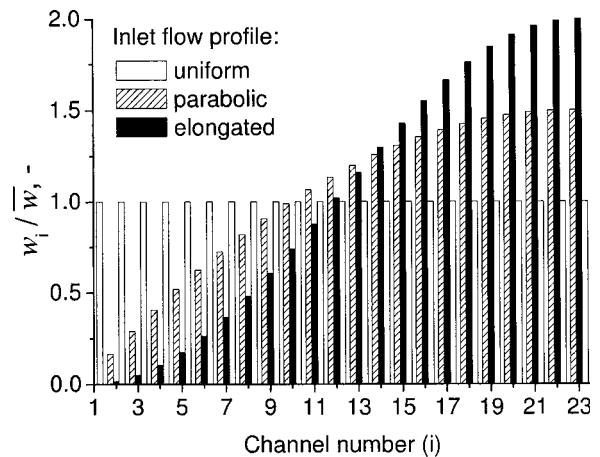
Two parameters are introduced herein to evaluate the differences in the flow distribution at the outlet of the downstream channels, that is, the relative outlet flow nonuniformity parameter to evaluate the flow differences between the elongated and uniform inlet profiles, expressed in the following equation:

$$R_j^{el} = 100 \frac{v_j^{el} - v_j^{un}}{\bar{v}} \quad (\%) \quad (11)$$

and between the parabolic and the uniform inlet profiles, expressed as

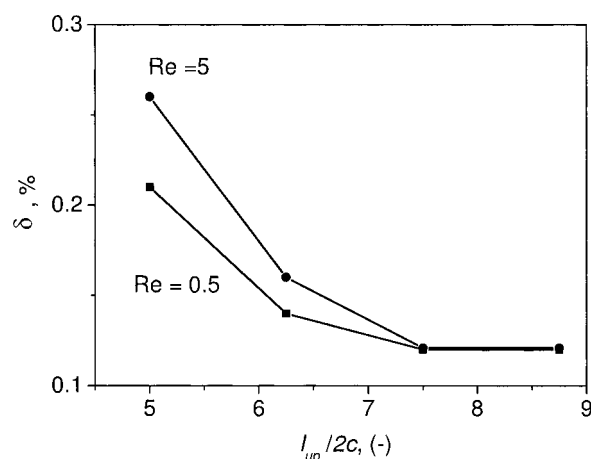
$$R_j^{par} = 100 \frac{v_j^{par} - v_j^{un}}{\bar{v}} \quad (\%) \quad (12)$$

Figure 4 presents the numerical results for a  $[45 \times 38]$  screen with  $a = 400 \mu\text{m}$ ,  $b = 260 \mu\text{m}$ ,  $c = 400 \mu\text{m}$ ,  $d = 400 \mu\text{m}$ ,  $h = 400 \mu\text{m}$ ,  $l_{up}/2c = 7.5$ , and  $l_{down}/2d = 7.5$ . One can see that the largest differences are observed in the outermost channels.



**Figure 2. Three different inlet flow profiles (elongated, parabolic, and uniform) assigned to the inlets of the upstream channels of the  $[45 \times 38]$  screen.**

The values are given only for a half of the geometry because of the symmetry.



**Figure 3. Flow nonuniformity (Eq. 10) as a function of the relative length of the upstream channels ( $l_{up}^*$ ) at Re of 0.5 and 5.**

$l_{up}^*$  is the ratio of the length of the upstream channel ( $l_{up}$ ) to the hydraulic diameter of the inlet flow duct of the screen.

Furthermore, two parameters, referred to as overall outlet flow nonuniformity parameters, were introduced to compare the differences between the elongated and the uniform (Eq. 13), as well as between the parabolic and the uniform cases (Eq. 14) in different screen configurations. These parameters were evaluated in a wide range of screen parameters:

$$\chi^{el} = \frac{100}{n\bar{v}} \sum_{j=1}^n |v_j^{el} - v_j^{un}| \quad (\%) \quad (13)$$

$$\chi^{par} = \frac{100}{n\bar{v}} \sum_{j=1}^n |v_j^{par} - v_j^{un}| \quad (\%) \quad (14)$$

The  $\chi^{el}$  and  $\chi^{par}$  values are listed in Table 2 for the lowest and highest values of design parameters. It is clear that the values of chosen objective functions are  $<0.02\%$  for a wide range of applied design parameters. Based on those results it can be concluded that the outlet flow distribution depends only on geometry parameters of the thick-walled screen and does not depend on the inlet distribution at the entrance to the upstream channels of the screen. Therefore, instead of complete modeling of the cone diffuser with the thick-walled screen, a prescribed parabolic flow profile (Eq. 8) was specified at the inlet of the upstream channels. Uniform static pressure of 101.3 kPa was specified at all outlets of the downstream channels. The range of flow velocities studied corresponds to a Reynolds number of 0.5–10. The pressure drop across the screen was always  $<1.0$  Pa.

### Optimization of the Header Configuration

At low Reynolds number, the flow is laminar. In this regime there is a linear flow resistance relation between the pressure drop ( $\Delta p$ ) along the channel and the volumetric flow rate ( $Q$ ) through the channel, expressed as

$$Q = G\Delta p \quad (15)$$

where  $G$  is a hydraulic conductance. At the interface between the upstream and downstream channels, flow is split up and further redistributed in the downstream channels (Figure 5). To compare the hydraulic resistance of different parts of the thick-walled screen, the entire geometry of the screen was decomposed into even portions. In this approach, the topmost and bottommost portions of upstream channels can be merged together to form a rectangle with height  $z_{V1}$ , whereas the middle part can be considered as parallel plates with height  $z_{V2}$ . For the screen applied:  $z_{V1} = 2(0.5a + b + d)$  and  $z_{V2} = 2(a + d)$ . Obviously, there is a difference in the hydraulic conductance for the fluid flow between the side and the middle portions of upstream channels represented in the present model by rectangular and parallel plates, respectively. Therefore, to determine the flow rate by the rectangular- and parallel-plate geometry, it is necessary to calculate their hydraulic conductances, for which the pressure drops are identical.

In the present analysis, instead of the actual velocity field entering each downstream channel from the upstream channels, an average value has been taken for the entire downstream channel ( $Q_{dwn}$ ). This average value depends on the mean velocity over a corresponding part of an upstream channel ( $Q_{up}$ ) and the  $b/a$  ratio of the thick-walled screen. To provide a uniform flow distribution in all the downstream channels, volumetric flow rate  $Q_{dwn1}$  has to be equal to  $Q_{dwn2}$  and so on. Because of the symmetry of the screen only half of the geometry of the downstream channels has to be considered. In our previous study, a methodology was presented for flow equalization by application of a thick-walled screen in which the  $b/a$  ratio was changed from 0 to 1.<sup>19</sup> It was observed that the ratio between the flow rate in the first and the second downstream channels is equal to the ratio of the volumetric flow rates by corresponding cross section of the upstream channel times the height of the corresponding cross sections:

$$\frac{Q_{dwn1}}{Q_{dwn2}} = \frac{Q_{up1} z_{up1}}{Q_{up2} z_{up2}} \quad (16)$$

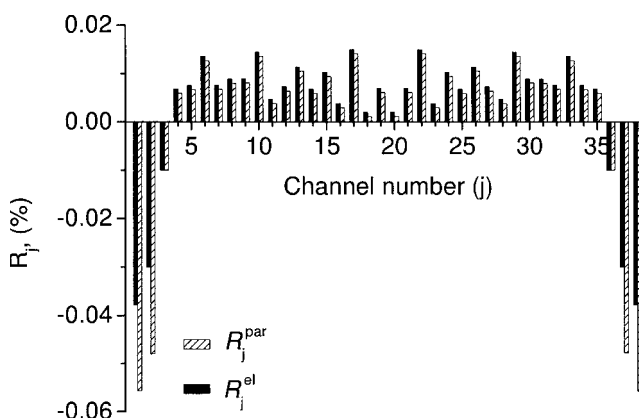


**Figure 4. Effect of upstream flow profile on the flow differences at the outlets of the downstream channels of the [45 × 38] screen.**

Parameters values:  $a = 400 \mu\text{m}$ ,  $b = 260 \mu\text{m}$ ,  $c = 400 \mu\text{m}$ ,  $d = 400 \mu\text{m}$ ,  $h = 400 \mu\text{m}$ ,  $l_{up}^* = 7.5$ , and  $l_{dwn}^* = 7.5$ .  $Re = 5$ .

**Table 2. Flow Nonuniformity Parameters  $\chi^{el}$  and  $\chi^{par}$  as a Function of Screen Design Parameters  $a$ ,  $c$ , and  $h^*$**

Average Reynolds Number in the Upstream Channels	Design Parameters ( $\mu\text{m}$ )			Objective Functions (%)	
	$a$	$c$	$h$	$\chi^{el}$	$\chi^{par}$
0.5	125	400	400	0.012	0.011
0.5	750	400	400	0.014	0.012
5	125	400	400	0.012	0.011
5	750	400	400	0.014	0.012
0.5	400	300	400	0.010	0.010
0.5	400	800	400	0.012	0.012
5	400	300	400	0.015	0.015
5	400	800	400	0.015	0.015
0.5	400	400	800	0.012	0.010
5	400	400	800	0.014	0.011

\*See Eqs. 13 and 14. Screen geometry:  $[22] \times [8]$ . The following parameters were kept constant:  $d = 400$  mm;  $l_{up}^* = 7.5$ ;  $l_{down}^* = 7.5$ ;  $Re = 5$ .

The correction factor counts for the pressure losses when the fluid moves from the upstream channels to the downstream channels of the screen. The reason for the correction factor can be understood if one observes the flow lines near the interface between the upstream and downstream channels (Figure 6a). For the case described in Mies et al.,<sup>19</sup> when  $b = 0.5a$  flow  $Q_{up1}$  is less than  $Q_{up2}$ , according to the CFD results, flow separation in upstream channels occurs above equidistant plane A12 between the first and second downstream channels. As a result, more fluid goes to the second downstream channel and less to the first one. This arises from the presence of an external wall, which creates an additional resistance to the fluid flow. To distribute flow equally, an additional room for flow distribution has to be created by increasing the area of the rectangle comparing to the area of the parallel plates or, in other words, increasing the  $b/a$  ratio to a certain value that is always  $>0.5$ .<sup>19</sup>

If the flow is equally distributed between the first and second downstream channels, flow separation between all subsequent downstream channels would always occur in corresponding equidistant planes (A23, A34, etc.) between the adjacent downstream channels (see Figure 6b) as a result of the symmetry of the thick-walled screen geometry. Therefore, the problem of flow equalization in a thick-walled screen at low Re numbers reduces to that of flow equalization in the

first and second downstream channels. In other words, the flow by the rectangular- and parallel-plate parts of the upstream channels times their height ratio has to be identical:

$$\frac{0.5a + b + d}{a + d} \frac{Q_{up1}}{Q_{up2}} = 1 \quad (17)$$

For isothermal, steady, incompressible flow of a Newtonian fluid through a duct of the arbitrary cross section, the product of the Fanning friction factor  $f_F$  and the Reynolds number is a constant—the Poiseuille number, Po:

$$Po = f_F Re \quad (18)$$

where  $f_F = 2\tau_w/\rho\bar{v}$ ,<sup>13</sup> and  $\bar{v} = \frac{1}{A} \int_A v dA$ ,  $\bar{v}$  is the cross-sectional average velocity, and  $\rho$  is the density. The mean wall shear stress  $\tau_w$  is defined as

$$\tau_w = \frac{D_h dp}{4 dl} \quad (19)$$

where  $D_h = 4A/P$  ( $A$  is channel cross-sectional area of the upstream channel and  $P$  is the upstream channel perimeter).

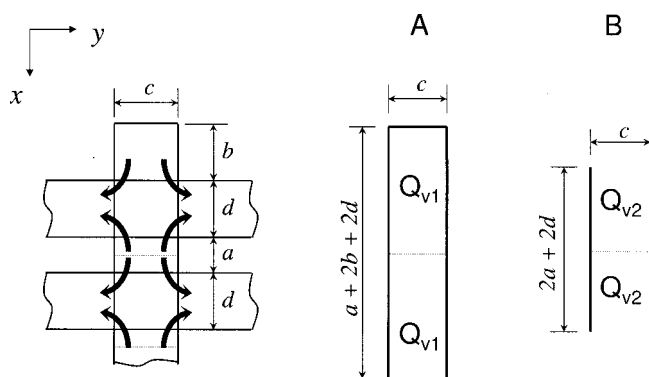


**Figure 5. Decomposition of the upstream channel geometry into regular pieces.**

(A) Two half rectangles merged together and (B) parallel plates.

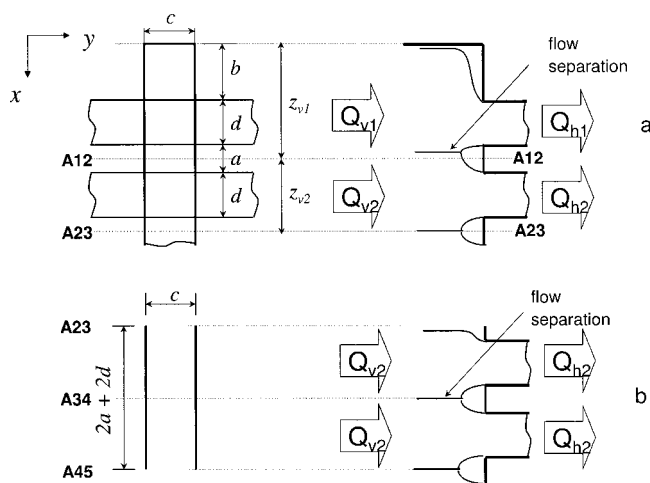


**Figure 6. Streamlines for the topmost (bottommost) and middle sections.**

A front view of the elementary units of the upstream screen is shown on the left. A cross-sectional view through the centerline of the screen near the interface between the upstream and downstream units is shown on the right.

By combining Eqs. 18 and 19 we can write the Poiseuille number in terms of experimental quantities:

$$Po = \frac{AD_h^2 \Delta p}{2\eta l_{up} Q} \quad (20)$$

where  $D_h$  is the hydraulic radius of an individual upstream channel,  $\Delta p$  is the pressure drop over the upstream channel length  $l_{up}$ ,  $\eta$  is the viscosity of the fluid, and  $Q = \bar{v}A$ . By comparing Eqs. 15 and 20, one may conclude

$$G = \frac{AD_h^2}{2l_{up}\eta Po} \quad (21)$$

The Poiseuille number for developing flow is defined as<sup>20</sup>

$$Po(t, x^+) = \frac{3.44}{\sqrt{x^+}} + \frac{0.674 + 1.3061t + 0.1222t^2 - 0.6718t^3}{4x^+} + 24P(t) - \frac{3.44}{\sqrt{x^+}} + \frac{2.9 \times 10^{-5} + 7.0 \times 10^{-5}t + 9.7 \times 10^{-4}t^2 - 7.8 \times 10^{-4}t^3}{1 + (x^+)^2} \quad (22)$$

where  $P(t) = 1 - 1.3553t + 1.9467t^2 - 1.7012t^3 + 0.9564t^4 - 0.2537t^5$ ;  $t$  is the aspect ratio,  $t = c/[a + 2(b + d)]$ ; and  $x^+$  is the dimensionless length. The  $Po$  number depends on both the channel aspect ratio and the dimensionless length of the upstream channels. By combining Eqs. 15 and 21, and assuming that viscosity of the fluid is identical in both channels, Eq. 17 can be rewritten as

$$\frac{0.5a + b + d}{a + d} \times \frac{A_{up1} D_{h-up1}^2 Po_{up2}}{A_{up2} D_{h-up2}^2 Po_{up1}} = 1 \quad (23)$$

where

$$A_{up1} = (0.5a + b + d)2c \quad A_{up2} = (a + d)2c$$

$$D_{h-up1} = \frac{(a + 2b + 2d)2c}{a + 2b + c + 2d}$$

and  $D_{h-up2} = 2c$ . Substituting the values for the cross-sectional areas and the hydraulic diameters into Eq. 23 yields, for flow equalization,

$$\frac{(a + 2b + 2d)^4}{(a + 2b + c + 2d)^2 (2a + 2d)^2} \frac{Po_{up2}}{Po_{up1}} = 1 \quad (24)$$

Therefore, at fixed values of design parameters  $a$ ,  $c$ ,  $d$ , and  $x^+$  the  $b/a$  ratio has to be found for which the value of the response function ( $f$ ) is equal to unity:

$$f = \frac{Q_{down1}}{Q_{down2}} = \frac{(a + 2b + 2d)^4}{(a + 2b + c + 2d)^2 (2a + 2d)^2} \frac{Po_{up2}}{Po_{up1}} \quad (25)$$

### Validation of the Approach for the Design of a Thick-Walled Screen

To assess the validity of the thick-walled screen mathematical model, the design results obtained by using this

model are compared with CFD simulation results, carried out by use of FLUENT<sup>®</sup> 6.0. The model predictions obtained at  $a = 250 \mu\text{m}$ ,  $c = 300 \mu\text{m}$ ,  $d = 2000 \mu\text{m}$ , and  $x_{up}^+ = 0.9$  were compared with the CFD results reported in Mies et al.,<sup>19</sup> where the geometry of the diffuser module was similar to that of a thick-walled screen. Figure 7 shows the  $f$ -values as a function of parameter  $a$  for three different  $b/a$  ratios of 0.0, 0.8, and 1.0 applied in Mies et al.<sup>19</sup> Symbols represent the  $f$ -values calculated based on the CFD results for the flow distribution between downstream channels 1 and 2. One can observe the rather good agreement between the CFD results and model predictions for all three cases. Furthermore, it can be seen from Figure 7 that the optimum  $b/a$  ratio becomes lower at larger distances between downstream channels and vice versa. One can conclude that increasing the separation between the downstream channels shifts the optimum  $b/a$  ratio to lower values. Figure 8a demonstrates that, as the  $b/a$  ratio increases, more flow goes by the topmost and the bottommost downstream channels. There is a minimum in flow nonuniformity ( $\delta = 0.120\%$ ) at a  $b/a$  ratio of 0.75 (Figure 8b). Both lower  $b/a$  of 0.73 and higher  $b/a$  of 0.77 ratios gave larger values of flow nonuniformity of 0.160 and 0.435%, respectively. CFD simulations give optimum  $b/a$  ratios of 0.75 and 0.62 for  $a = 250$  and  $500 \mu\text{m}$ , respectively, whereas other design parameters are fixed at the following values:  $c = 300 \mu\text{m}$ ,  $d = 400 \mu\text{m}$ , and  $x_{up}^+ = 0.4$ . Predictions made by the present model give optimum values of 0.759 and 0.628, respectively. Thus, there is hardly any difference between results of both designs. The proposed model can be applied for the design of a screen in a wide range of design parameters.

### Effect of Design Parameters on Flow Nonuniformity

#### Effect of the number of the upstream channels ( $m$ )

The effect of the number of upstream channels was investigated over a cross section of 12.9 mm (width)  $\times$  16 mm (height) by comparing the  $\delta$ -values obtained in the  $[22 \times 8]$  screen with those obtained in the  $[11 \times 8]$  and  $[8 \times 8]$  geo-

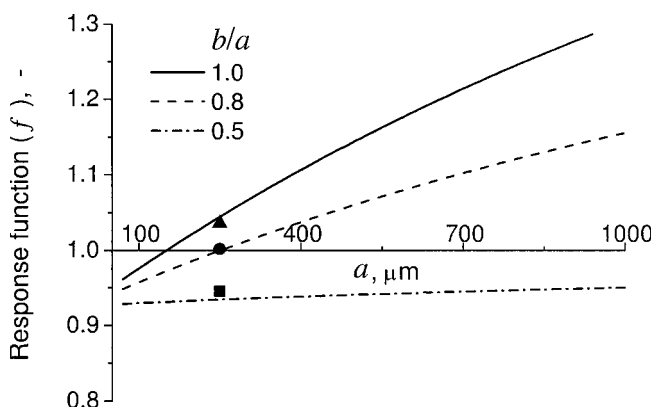


Figure 7. Response function  $f$  as a function of distance between the downstream channels for three different  $b/a$  ratios: 0.5, 0.8, and 1.0.

Symbols represent corresponding CFD data.

metries (Figure 9). In the latter cases, parameter  $h$  was increased from 300 to 960 and 1500  $\mu\text{m}$ , respectively, other parameters being identical to those mentioned in the beginning of this section. The cross section represents a quarter of the geometry arising from the symmetry. The results were found to be independent of the flow rate with respect to Re numbers ranging from 0.5 to 10.

Increasing the number of upstream channels ( $m$ ) from 8 to 11 decreases the flow nonuniformity while the optimum  $b/a$  ratio remains the same. Further increase of the number of the upstream channels from 11 to 22 does not improve the flow distribution at the outlets of the downstream channels of the screen. This leads to the conclusion that there is an optimum number of upstream channels per unit width of a thick-walled screen beyond which flow nonuniformity remains virtually constant. This number corresponds to one upstream channel per a length of 1260  $\mu\text{m}$  in the  $y$ -direction (see Figure 1). In other words, eight upstream channels are required per 1 cm of width of a thick-walled screen to provide a flow nonuniformity  $< 0.2\%$ . A larger number of channels would considerably hamper the manufacturing of the device, and therefore must be avoided. It should be noted that increasing parameter  $a$  from 250 to 500  $\mu\text{m}$  shifts the optimum  $b/a$  ratio to the lower values (Figure 9). However, it does not change either the optimum number of upstream channels or the optimum value of the flow nonuniformity parameter ( $\delta$ ). The effect of the  $b/a$  ratio on the flow distribution at the downstream channels becomes less important for a screen consisting of a large number of downstream channels ( $n > 100$ ); however, it plays an important role for the screens with a medium ( $10 < n < 100$ ) and it is more dominant for small number of downstream channels ( $n < 10$ ).

#### Effect of the wall thickness between two neighboring downstream channels ( $a$ )

From the discussion in the previous section, it becomes clear that as parameter  $a$  increases, the  $b/a$  ratio has to be reduced to obtain flow equalization in the whole range of values of parameter  $a$ . Therefore, the problem can be formu-

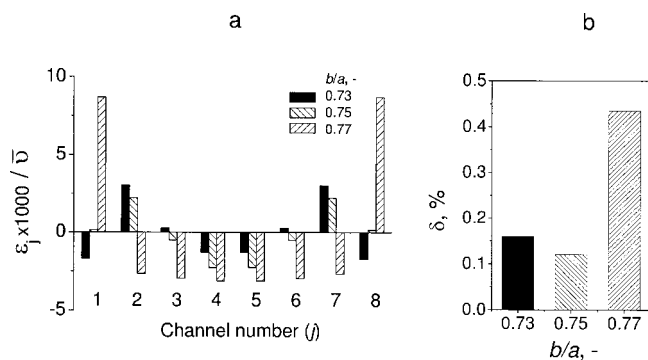


**Figure 8. (a) Flow difference in the downstream channels relative to the mean flow in all downstream channels of the  $[22 \times 8]$  screen as a function of the  $b/a$  ratio; (b) flow nonuniformity ( $\delta$ ) as a function of the  $b/a$  ratio.**

Parameters values:  $a = 250 \mu\text{m}$ ,  $c = 300 \mu\text{m}$ ,  $h = 300 \mu\text{m}$ ,  $d = 2 \text{ mm}$ ,  $l_{up} = 7.5$ , and  $l_{down} = 7.5$ .  $Re = 5$ .

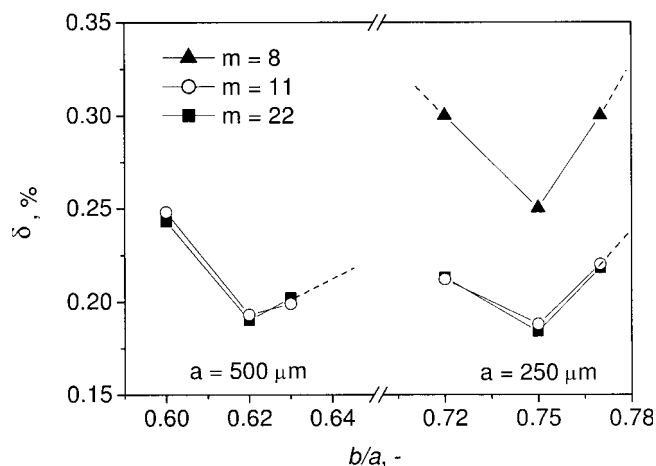


**Figure 9. Effect of the number of the upstream channels ( $m$ ) on the flow nonuniformity at  $a = 250$  and  $500 \mu\text{m}$  and different  $b/a$  ratios.**

Screen geometries of  $[22 \times 8]$ ,  $[11 \times 8]$ , and  $[8 \times 8]$  were applied over a cross section of 12.9 mm (width)  $\times$  16 mm (height), corresponding to parameter  $h$  of 300 to 960 and 1500  $\mu\text{m}$ , respectively. Other screen parameters were the same as those in Figure 7.

lated as finding an optimum function that minimizes the flow nonuniformity index  $\Omega$ , defined as

$$\Omega = \left[ \frac{1}{a_2 - a_1} \int_{a_1}^{a_2} \frac{(a + 2b + 2d)^4}{(a + 2b + c + 2d)^2 (2a + 2d)^2} \frac{Po_{up2}}{Po_{up1}} da \right] - 1 \quad (26)$$

The index  $\Omega$  is the average value of the response function  $f$  on the interval of values  $a$  between  $a_1 = 100 \mu\text{m}$  and  $a_2 = 1000 \mu\text{m}$ , which are within interest for microreactor applications. Several functions with two fitting parameters can be used to describe the ensemble of data points generated by the screen model. In their discrimination, the following criteria were applied:

$$\Omega \leq 1 \times 10^{-5} \quad (27)$$

$$|f(a, b, c, d, x_{up}^+) - 1| \leq 0.005 \quad \text{for} \quad 100 \leq a \leq 1000 (\mu\text{m}) \quad (28)$$

The first criterion is set to minimize the flow nonuniformity in the whole range of values of parameter  $a$ . The second criterion states that at any given value of parameter  $a$ , the flow nonuniformity should not exceed 0.5%. To satisfy the constraints given by Eqs. 27 and 28, a function for the  $b/a$  ratio can be found in the form

$$\frac{b}{a} = P1 + \frac{P2}{a} \quad (29)$$

Figure 10 demonstrates two sets of  $f$ -function (see Eq. 25) plots: one at constant  $b/a$  ratio of 0.5 and one when the fitting function given by Eq. 29 was applied. It can be seen that the flow equipartition is achieved in the whole range of  $a$ -values for different values of parameters  $c$  and  $d$  if the  $b/a$  ratio is a function of the parameter  $a$ , and the fitting param-



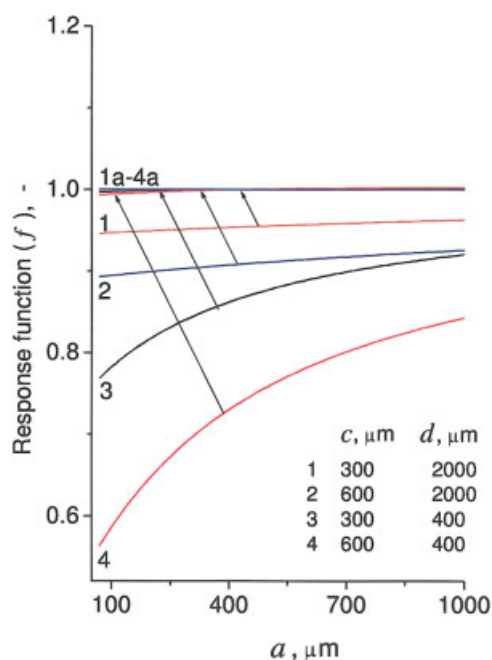


**Figure 10.** Response function  $f$  as a function of distance between the downstream channels.

Curves 1–4 are obtained at  $b/a = 0.5$ . Curves 1a–4a are obtained with the fitting function given by Eq. 29. [Color figure can be viewed in the online issue, which is available at [www.interscience.wiley.com](http://www.interscience.wiley.com).]

ters  $P1$  and  $P2$  are properly chosen (see Table 3). It can be seen from Table 3 that the parameter  $P1$  is always 0.5, whereas parameter  $P2$  depends on parameter  $c$  and, to a lesser extent, on parameter  $d$ . Therefore, the fitting function can be rewritten as follows:

$$b = 0.5a + P2 \quad (30)$$

Equation 30 shows that parameter  $P2$  can be neglected if  $a \gg 2P2$ . If the value of parameter  $a$  exceeds the  $P2$  value by 20-fold, the contribution of the latter parameter is  $<10\%$ . Therefore,  $P2$  can be neglected if  $a > 2.3$  mm because maximum values of parameter  $P2$  are found to be about 115  $\mu\text{m}$  (see Table 3). This is a typical situation for monolith reactors. However, microreactors have a typical separation between the adjacent sets of channels ( $a$ ) of  $<1$  mm, at which the contribution of  $P2$  is rather substantial. A complete analysis of the dependency of parameter  $P2$  on the design parameters of the screen is beyond the scope of the present study and is reported elsewhere.<sup>21</sup>

**Table 3.** Fitting Parameters  $P1$  and  $P2$  for the Parameter  $b$ :  $b(a) = P1a + P2^*$

$c, \mu\text{m}$	$d, \mu\text{m}$	$P1$	$P2, \mu\text{m}$
300	400	0.500	57.00
300	2000	0.500	56.65
600	400	0.500	115.8
600	2000	0.500	113.4

\*The dimensionless length of the upstream channels equals 0.9.

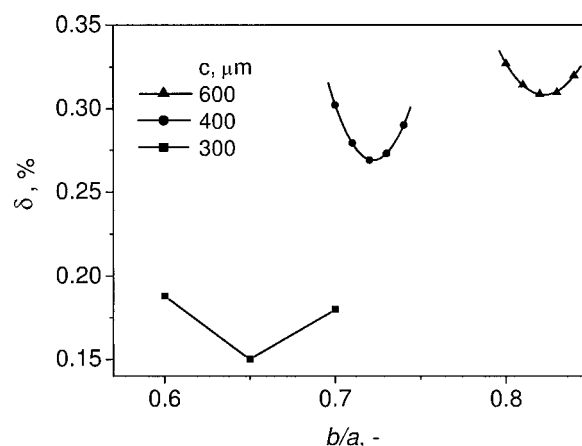


**Figure 11.** Flow nonuniformity ( $\delta$ ) as a function of  $b/a$  ratio at different values of parameter  $c$ : 300, 400, and 600  $\mu\text{m}$ .

Screen geometry of  $[11 \times 8]$  was applied over a cross section of 12.9 mm (width)  $\times$  17.2 mm (height). Parameters values:  $a = 400$   $\mu\text{m}$ ,  $d = 2$  mm, and the sum of parameters  $c$  and  $h$  was kept constant at 1260  $\mu\text{m}$ . Other screen parameters were the same as those in Figure 7.

#### Effect of the width of the upstream channels ( $c$ )

The width of the upstream channels ( $c$ ) was varied over a cross section of 12.9 mm (width)  $\times$  17.2 mm (height) in the  $[11 \times 8]$  geometry in the range between 300 and 600  $\mu\text{m}$  to investigate its effect on the flow nonuniformity. In this study,  $l_{up}^* = 7.5$ ,  $a = 400$   $\mu\text{m}$ ,  $d = 2$  mm, and the sum of parameters  $c$  and  $h$  was kept constant at 1260  $\mu\text{m}$ . When the width of the upstream channel increases from 300 to 600  $\mu\text{m}$ , a minimum flow nonuniformity doubles from 0.155 to 0.31%, whereas the optimum  $b/a$  ratio shifts to the higher values (Figure 11). The range of  $b/a$  ratios satisfying the design criteria, acceptable in most studies ( $\delta < 0.5\%$ ), becomes more narrow at  $c = 600$   $\mu\text{m}$ . A typical precision of micromachining is 10  $\mu\text{m}$ , which can prompt a shift in the  $b/a$  ratio of  $\pm 0.02$ . For example, at  $c = 600$   $\mu\text{m}$ , the optimum  $b/a$  ratio equals 0.82 ( $b = 328$   $\mu\text{m}$ ) corresponding to the flow nonuniformity of 0.31%. When the screen is not properly assembled (such as  $b = 338$   $\mu\text{m}$ ), the  $\delta$ -value would be 0.33%, generating an increase in the flow nonuniformity of 0.02%. Therefore, the width of upstream channels ( $c$ ) can be safely set at 600  $\mu\text{m}$  unless very low values of flow nonuniformity ( $\delta < 0.15\%$ ) are desired. The values  $> 600$   $\mu\text{m}$  can also be applied. This, in turn, would require a longer length of the screens to satisfy the criterion:  $l_{up}^* = 7.5$ .

#### Conclusions

An original design of a flow distribution header, consisting of a cone diffuser and a thick-walled screen, is proposed for equalizing flow distribution in microstructured reactors having constraints related to flow uniformity and pressure drop. In this design, the degree of flow nonuniformity does not depend on the flow distribution entering the thick-walled screen and is defined by the geometry of the thick-walled screen itself. The diffuser expansion angle plays no role in

equalizing the fluid flow. Therefore, it is recommended to use the diffusers with expansion angle close to  $180^\circ$  (sudden expansion) to minimize the dead volume of the header. The problem of flow equalization in a thick-walled screen at low Reynolds numbers reduces to that of flow equalization in the first (topmost) and second downstream channels of the thick-walled screen. In turn, this requires flow equalization in the corresponding cross sections of upstream channels, which can be modeled by rectangular- and parallel-plate geometries. The influence of different design parameters of a thick-walled screen on the flow nonuniformity has been analyzed by performing a CFD study. At least eight upstream channels with a width of  $300\text{ }\mu\text{m}$  are required per 1 cm of width of a thick-walled screen to provide a flow nonuniformity  $< 0.2\%$ . The width of the upstream channels can be increased to  $600\text{ }\mu\text{m}$ . However, this will double the flow nonuniformity and will shift the optimum distance between a top wall of the topmost downstream channel and a side wall of the upstream channel to higher values. The proposed screen configuration can minimize the ratio of the maximum flow velocity to the minimum flow velocity from 2 to 1.005 for a wide range of Reynolds numbers, which in turn can improve the performance of a downstream microreactor.

## Acknowledgments

The financial support by the Dutch Technology Foundation (STW, Project No. EPC.5543) by the Netherlands Organization for Scientific Research and (NWO) and the Russian Foundation for Basic Research (RFBR), Project No. 047.015.007, is gratefully acknowledged.

## Notation

$A$  = cross-sectional area of a fluid channel,  $\text{m}^2$   
 $a$  = distance between two neighboring downstream channels, m  
 $b$  = distance in cross-sectional view between a top wall of the first downstream channel and a side wall of the upstream channel, m  
 $c$  = width of the upstream channels, m  
 $d$  = height of the downstream channels, m  
 $D_h$  = hydraulic diameter ( $=4A/P$ ), m  
 $f_F$  = fanning friction factor ( $=2\tau_w/\rho v^2$ )  
 $F$  = open cross section,  $\text{m}^2$   
 $G$  = hydraulic conductance ( $=AD_h^2/2l_{up}\eta\text{Po}$ ),  $\text{m}^4\text{ s kg}^{-1}$   
 $h$  = distance between two neighboring upstream channels, m  
 $l$  = channel length, m  
 $l^*$  = relative length (the length to hydraulic diameter ratio) ( $=l/D_h$ )  
 $m$  = number of the upstream channels  
 $N_0$  = Coriolis's coefficient (a ratio of true kinetic energy to kinetic energy calculated based on average flow velocity) ( $=\int_{A_0} w^3 dA/w_0^3 A_0$ )  
 $n$  = number of the downstream channels  
 $P$  = perimeter of the channel, m  
 $\Delta p$  = pressure drop,  $\text{kg m}^{-1}\text{ s}^{-2}$   
 $\text{Po}$  = Poiseuille number ( $=AD_h^2\Delta p/2\eta l_{up}Q$ )  
 $R_j^*$  = relative flow difference parameter, % ( $[(v_j^* - v_j^{un})/\bar{v}] \times 100$ ). It compares the flow difference in the downstream channels when a prescribed flow profile ( $^* = \text{par}, \text{el}$ ) was applied in the upstream channels instead of the uniform profile.  
 $\text{Re}$  = Reynolds number ( $=\bar{v}\rho D_h/\eta$ )  
 $Q$  = volumetric flow rate ( $=\bar{v}A$ ),  $\text{m}^3\text{ s}^{-1}$   
 $t$  = aspect ratio  
 $v_j$  = area-averaged velocity at the outlet of downstream channels  $j$ , m/s  
 $\bar{v}$  = mean velocity over all outlets of the downstream channels, m/s  
 $w$  = velocity in the upstream channels, m/s  
 $\bar{w}$  = mean inlet velocity over all upstream channels, m/s  
 $x^+$  = dimensionless length of the channel ( $=l/D_h\text{Re}$ )  
 $z$  = height of a upstream channel, m

## Greek letters

$\alpha$  = expansion angle of the flow diffuser,  $^\circ$   
 $\delta$  = flow nonuniformity index ( $=(100/\bar{v}) \times [\sum_{j=1}^n (v_j - \bar{v})^2]/(n-1)$ ), %  
 $\chi^*$  = overall outlet flow difference parameter ( $=(100/n\bar{v}) \times \sum_{j=1}^n |v_j^* - v_j^{un}|$ ), %. It compares the flow difference in the downstream channels when a prescribed flow profile ( $^* = \text{par}, \text{el}$ ) was applied in the upstream channels instead of the uniform profile.  
 $\varepsilon_j$  = flow difference in channel  $j$  relative to the mean flow in all downstream channels ( $=v_j - \bar{v}$ )  
 $\eta$  = fluid viscosity,  $\text{kg m}^{-1}\text{ s}^{-1}$   
 $v$  = cross-sectional average velocity ( $=(1/A) \int_A v dA$ ),  $\text{m s}^{-1}$   
 $\rho$  = fluid density,  $\text{kg/m}^3$   
 $\Omega$  = flow nonuniformity index ( $=(1/(a^2 - a^1)) \int_{a^1}^{a^2} f da - 1$ )  
 $\zeta$  = drag coefficient of the screen  
 $\tau_w$  = mean wall shear stress ( $=(D_h/4)(dp/dl)$ ),  $\text{kg m}^{-1}\text{ s}^{-2}$

## Superscripts

$cr$  = critical  
 $opt$  = optimal  
 $el$  = elongated  
 $par$  = parabolic  
 $un$  = uniform

## Subscripts

$d$  = diffuser chamber  
 $dwn$  = downstream channels  
 $i$  = upstream channel number  
 $j$  = downstream channel number  
 $o$  = inlet flow duct  
 $rel$  = relative  
 $max$  = maximum  
 $sc$  = screen  
 $up$  = upstream channel  
 $1$  = above the A12 plane  
 $2$  = between the A12 and A23 planes

## Literature Cited

1. Rebrov EV, Duinkerke SA, de Croon MHJM, Schouten JC. Optimization of heat transfer characteristics, flow distribution, and reaction processing for a microstructured reactor/heat-exchanger for optimal performance in platinum catalyzed ammonia oxidation. *Chem Eng J.* 2003;93:201–216.
2. Commenge JM, Falk L, Corriou JP, Matlosz M. Optimal design for flow uniformity in microchannel reactors. *AIChE J.* 2002;48:345–358.
3. Ajmera SK, Delattre C, Schmidt MA, Jensen KF. Microfabricated differential reactor for heterogeneous gas phase catalyst testing. *J Catal.* 2002;209:401–412.
4. Amador C, Gavrilidis A, Angeli P. Flow distribution in different microreactor scale-out geometries and the effect of manufacturing tolerances and channel blockage. *Chem Eng J.* 2004;101:379–390.
5. Tonomura O, Tanaka S, Noda M, Kano M, Hasebe S, Hashimoto I. CFD-based optimal design of manifold in plate-fin microdevices. *Chem Eng J.* 2004;101:397–402.
6. Ranganayakulu C, Seetharamu KN. The combined effects of wall longitudinal heat conduction, inlet fluid flow nonuniformity and temperature nonuniformity in compact tube-fin heat exchangers: A finite element method. *Int J Heat Mass Transfer.* 1999;42:263–273.
7. Jiao A, Baek S. Effects of distributor configuration on flow maldistribution in plate-fin heat exchangers. *Heat Transfer Eng.* 2005;26:19–25.

8. Prabhakara RB, Krishna KP, Das SK. Effect of flow distribution to the channels on the thermal performance of a plate heat exchanger. *Chem Eng Proc.* 2002;41:41–58.
9. Idelchik IE. *Handbook of Hydraulic Resistance*. Boca Raton, FL: CRC Press; 1994.
10. Idelchik IE. *Fluid Dynamics of Industrial Equipment: Flow Distribution Design Methods*. London: Hemisphere; 1991.
11. Taganov GI. Equalizing performance of grids in gas and liquid flows. *Trans TsAGI.* 1947;604:14.
12. Riman IS. Modification of velocity profiles in variable cross section ducts by placement of meshes. *Promyshlennaya Aerodin. (Ind Aerodyn).* 1960;20:216–238.
13. Taylor GI, Batchelor GK. The effect of wire gauze on small disturbances in a uniform stream. *J Mech Appl Math.* 1949;11:1–29.
14. Riman IS, Cherepkova VG. An approximate method for calculation of flow field in a tube filled with thick-walled bars. *Ind Aerodyn.* 1973;30:65–74.
15. *FLUENT Users Guide*. Lebanon, NH: Fluent Inc.; 2005.
16. Mies MJM, Rebrov EV, Deutz L, Kleijn CR, de Croon MHJM, Schouten JC. Experimental validation of the performance of a microreactor for the high-throughput screening of catalytic coatings. *I&EC Res.* 2007, in press.
17. Mies MJM, Rebrov EV, de Croon MHJM, Schouten JC, Ismagilov IZ. *Inlet Section for Micro-Reactor*. Patent PCT/NL2006/050074; 2006.
18. Idelchik IE, Ginzburg YaL. Main results of experimental investigations of conical diffusers. In: *Scrubbing of Industrial Gases*. Moscow: Mashinostroenie; 1974.
19. Mies MJM, Rebrov EV, de Croon MHJM, Schouten JC. Design of a molybdenum high throughput micro-reactor for high temperature screening of catalytic coatings. *Chem Eng J.* 2004;101:225–235.
20. Shah RK, London AL. *Laminar Flow Forced Convection in Ducts*. New York: Academic Press; 1978.
21. Ekatpure RP, Rebrov EV, de Croon MHJM, Schouten JC. Optimization of design parameters of a thick-walled screen for flow equalization in microstructured reactors. *J Micromech Microeng.* 2007, in press.

*Manuscript received May 11, 2006, and revision received Sept. 22, 2006.*